Formation of Plasma Proto-Galaxies by Turbulent Fragmentation: Quasar Quartet Images of Young Chain-Cluster-Galaxies

Carl H. Gibson

University of California San Diego
Departments of MAE and SIO
Center for Astrophysics and Space Sciences
La Jolla, CA, 92093-0411
cgibson@ucsd.edu

ABSTRACT

Observations of four linearly-aligned, closely-spaced-quasars (Quasar Quartet) are explained (Hennawi et al. 2015) as the progenitor of an even more massive galactic structure. An alternative interpretation is that such linear structures reflect turbulent vortex lines of the plasma epoch, which are progenitors of chain-galaxy-clusters such as the Stephan Quintet and other Hickson compact groups of galaxies (Gibson and Schild 2007), where turbulence creates and stretches the line of galaxies into slender pencils viewed end on, aided by the expansion of the universe.

BACKGROUND

As Hennawi et al. 2015 point out, the odds of observing four quasars packed together in the size of a few present day galaxies is about one in 10^7 assuming the standard LCDMHC cosmology where galaxies are assembled star by star from gas and dust. Something is wrong with "current cosmological simulations" as said in their Abstract. The problem is with the assumptions of the simulations, which should be based on HGD cosmology to include collisional fluid mechanics and turbulence, as proposed by Gibson and Schild 2007 in their interpretation of a similar compact galaxy group called the Stephan Quintet. Viscous forces of the early plasma epoch prevent fragmentation of the plasma until the Schwarz viscous and turbulent scales become smaller than the Hubble scale of causal connection ct, where c is the light speed and t is the time.

CONCLUSIONS

The system observed is not the progenitor of a massive galaxy cluster as suggested in the Abstract of Hennawi et al. 2015. Instead, it is the progenitor of a chain-galaxy-cluster of galaxies such as Stephan Quintet. Eventually it will be stretched into a thin pencil by the expansion of the universe, as shown in the figure. Most, perhaps all, galaxies of the universe originated by fragmentation of viscous plasma along turbulent vortex lines, where the rate-of-strain γ is maximum, since L_{SV} is $\sim [\gamma\nu/\rho G]^{1/2}$, and the Reynolds number of the flow is small. Therefore, $L_{SV} \sim L_{ST}$. Viscous stresses of the plasma resist separation by the expansion of the universe until $L_{SV} \sim ct$, permitting the evolution of nearby galaxies to reach quasar brightness before they are separated. Recall that the

kinematic viscosity ν of the plasma is large ($3x10^{26}$ m^2 s^{-1}) and the density ρ is small ($3x10^{-17}$ kg m^{-3}), giving $L_{SV} \sim 10^{20}$ m at $t \sim 10^{12}$ s (Gibson 1996).

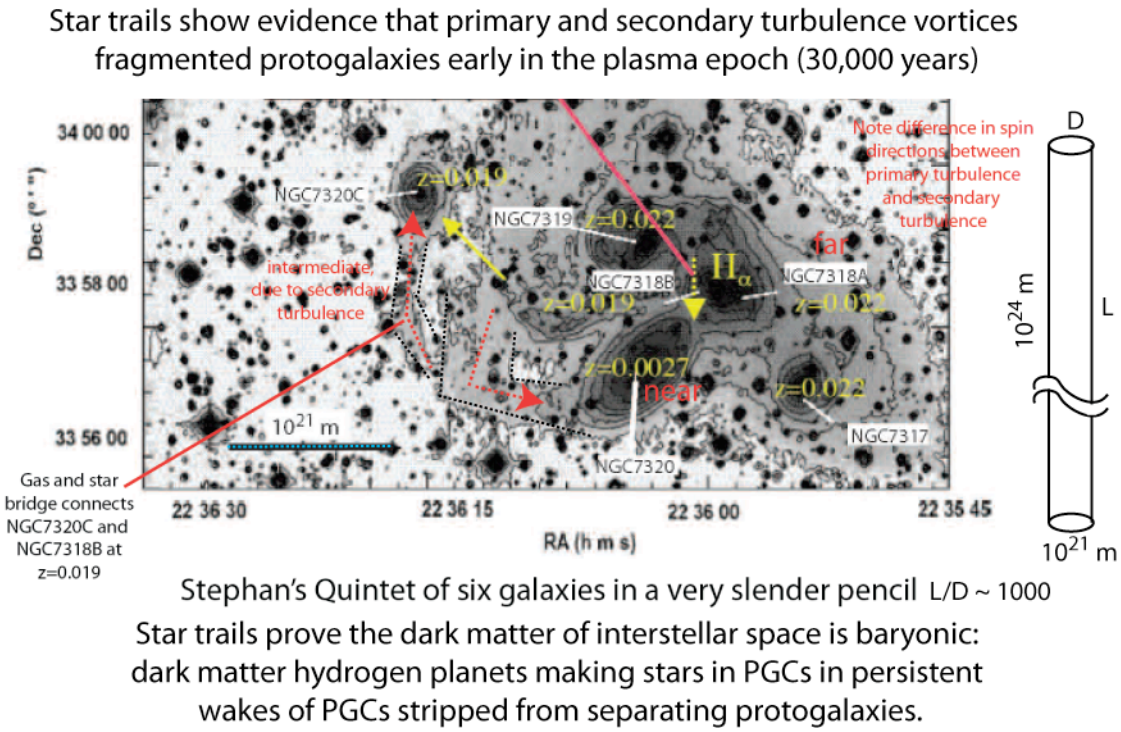

Figure JC2015.24.45.2, by Carl H. Gibson. Star trails to NGC7320C from NGC318B, both galaxies at red shift z = 0.019, show a clockwise turbulent eddy separated the two when they were plasma protogalaxies. Likewise, inertial vortex forces of the counter-clockwise primary turbulent eddy, and the expansion of the universe, separated NGC7320 (near) from the other protogalaxies (far) after plasma to gas transition (10^{13} s), to form the Stephan Quintet Hickson compact group. Dotted black lines outline the fossil turbulence star trail wakes of the separating galaxies. The galaxies are NOT "crashing together", as often stated in descriptions of the Stephan Quintet (by NASA etc.). Realize from HGD cosmology (Gibson 1996, Schild 1996), about ten Nomura Scale L_N (10^{20} m) plasma protogalaxies will fragment along a plasma turbulence vortex line at 30,000 years when these embryonic galaxies become possible. Physically, the Schwarz viscous, turbulent and Hubble (*ct*) length scales all approximately converge to the protogalaxy scale L_N when time *t* increases to ~10^{12} s, assuming constant light speed *c*. Note that *ct* at 10^{12} s is ~ 10^{20} m.

acts as a peculiar scatterer in phase space (5). Other cat-like states and squeezed states could then be produced. Tailoring the Hilbert space in time is an important new resource for quantum control. Our experiment enables the realization of various protocols based on QZD, such as generation and protection of entanglement (21–23), and quantum logic operations (24). Moreover, by turning on and off in time the blockade level and combining it with fast amplitude displacements, which is feasible by improving the cavity decay rate by an order of magnitude, it would be possible to realize phase space tweezers for light (4, 5). A possible and important outcome would then be the manipulation of Schrödinger cat states in a unique way and the quantum error correction of cat-qubits, which are a promising quantum computing paradigm (25).

REFERENCES AND NOTES

1. P. Facchi, V. Gorini, G. Marmo, S. Pascazio, E. C. G. Sudarshan, Phys. Lett. A 275, 12–19 (2000).
2. P. Facchi, S. Pascazio, Phys. Rev. Lett. 89, 080401 (2002).
3. P. Facchi, D. Lidar, S. Pascazio, Phys. Rev. A 69, 032314 (2004).
4. J. M. Raimond et al., Phys. Rev. Lett. 105, 213601 (2010).
5. J. M. Raimond et al., Phys. Rev. A 86, 032120 (2012).
6. B. Misra, E. C. G. Sudarshan, J. Math. Phys. 18, 756 (1977).
7. Originally, QZD corresponded to quantum evolutions restricted by measurement; the name was later extended to any quantum dynamics in a restricted Hilbert space (3).
8. F. Schäfer et al., Nat. Commun. 5, 3194 (2014).
9. A. Signoles et al., Nat. Phys. 10, 715–719 (2014).
10. D. I. Schuster et al., Nature 445, 515–518 (2007).
11. H. Paik et al., Phys. Rev. Lett. 107, 240501 (2011).
12. G. Kirchmair et al., Nature 495, 205–209 (2013).
13. Materials and methods are available as supporting materials on Science Online.
14. S. E. Nigg et al., Phys. Rev. Lett. 108, 240502 (2012).
15. J. Bourassa, F. Beaudoin, J. M. Gambetta, A. Blais, Phys. Rev. A 86, 013814 (2012).
16. F. Solgun, D. Abraham, D. P. DiVincenzo, Phys. Rev. B 90, 134504 (2014).
17. L. Lutterbach, L. Davidovich, Phys. Rev. Lett. 78, 2547–2550 (1997).
18. P. Bertet et al., Phys. Rev. Lett. 89, 200402 (2002).
19. B. Vlastakis et al., Science 342, 607–610 (2013).
20. S. Haroche, J. M. Raimond, Exploring the Quantum (Oxford Univ. Press, Oxford, 2006).
21. S. Maniscalco, F. Francica, R. L. Zaffino, N. Lo Gullo, F. Plastina, Phys. Rev. Lett. 100, 090503 (2008).
22. X-B. Wang, J. Q. You, F. Nori, Phys. Rev. A 77, 062339 (2008).
23. Z. C. Shi, Y. Xia, H. Z. Wu, J. Song, Eur. Phys. J. D 66, 127 (2012).
24. X-Q. Shao, L. Chen, S. Zhang, K-H. Yeon, J. Phys. B 42, 165507 (2009).
25. M. Mirrahimi et al., New J. Phys. 16, 045014 (2014).

ACKNOWLEDGMENTS

We thank M. Devoret, Ç. Girit, T. Kontos, Z. Leghtas, V. Manucharyan, M. Mirrahimi, S. Pascazio, the Quantronics Group, J. -M. Raimond, P. Rouchon, S. Dhillon, and J. Viennot. Nanofabrication has been made within the consortium Salle Blanche Paris Centre. This work was supported by the ANR contract ANR-12-JCJC-TIQS and the Qumotel grant Emergences of Ville de Paris. L.B. acknowledges support from Direction Générale de l'Armement.

SUPPLEMENTARY MATERIALS

www.sciencemag.org/content/348/6236/776/suppl/DC1
Materials and Methods
Supplementary Text
Figs. S1 to S4
References (26–32)

29 July 2014; accepted 3 April 2015
10.1126/science.1259345

GALAXY EVOLUTION This quintet of quasars is a baby picture of chain clusters of galaxies produced by turbulence in the plasma epoch at about 10^12 seconds. CHG

Quasar quartet embedded in giant nebula reveals rare massive structure in distant universe

Joseph F. Hennawi,[1]* J. Xavier Prochaska,[2] Sebastiano Cantalupo,[2,3] Fabrizio Arrigoni-Battaia[1]

This is NOT the progenitor of a massive galaxy cluster. It is the progenitor of a chain cluster of galaxies, like Stephan's Quintet. See Journal of Cosmology, Vol. 24.

All galaxies once passed through a hyperluminous quasar phase powered by accretion onto a supermassive black hole. But because these episodes are brief, quasars are rare objects typically separated by cosmological distances. In a survey for Lyman-α emission at redshift $z \approx 2$, we discovered a physical association of four quasars embedded in a giant nebula. Located within a substantial overdensity of galaxies, this system is probably the progenitor of a massive galaxy cluster. The chance probability of finding a quadruple quasar is estimated to be $\sim 10^{-7}$, implying a physical connection between Lyman-α nebulae and the locations of rare protoclusters. Our findings imply that the most massive structures in the distant universe have a tremendous supply ($\simeq 10^{11}$ solar masses) of cool dense (volume density $\simeq 1\ \mathrm{cm}^{-3}$) gas, which is in conflict with current cosmological simulations.

Cosmologists do not fully understand the origin of supermassive black holes (SMBHs) at the centers of galaxies and how they relate to the evolution of the underlying dark matter, which forms the backbone for structure in the universe. In the current paradigm, SMBHs grew in every massive galaxy during a luminous quasar phase, making distant quasars the progenitors of the dormant SMBHs found at the centers of nearby galaxies. Tight correlations between the masses of these local SMBHs and both their host galaxy (1) and dark-matter halo masses (2) support this picture, further suggesting that the most luminous quasars at high redshift (z) should reside in the most massive galaxies. It has also been proposed that quasar activity is triggered by the frequent mergers that are a generic consequence of hierarchical structure formation (3, 4). Indeed, an excess in the number of small-separation binary quasars (5, 6), as well as the mere existence of a handful of quasar triples (7, 8), support this hypothesis. If quasars are triggered by mergers, then they should preferentially occur in rare peaks of the density field, where massive galaxies are abundant and the frequency of mergers is highest (9).

Following these arguments, one might expect that at the peak of their activity, $z \sim 2$ to 3, quasars should act as signposts for protoclusters, the progenitors of local galaxy clusters and the most massive structures at that epoch. However, quasar clustering measurements (10, 11) indicate that quasar environments at $z \sim 2$ to 3 are not extreme: These quasars are hosted by dark-matter halos with masses $M_{\mathrm{halo}} \sim 10^{12.5}\ M_{\odot}$ (where $M_{\odot}$ is the mass of the Sun), too small to be the progenitors of local clusters (12). But the relationship between quasar activity and protoclusters remains unclear, owing to the extreme challenge of identifying the latter at high redshift. Indeed, the total comoving volume of even the largest surveys for distant galaxies at $z \sim 2$ to 3 is only $\sim 10^{7}\ \mathrm{Mpc}^{3}$, which would barely contain a single rich cluster locally.

Protoclusters have been discovered around a rare population of active galactic nuclei (AGNs) powering large-scale radio jets, known as high-redshift radio galaxies (HzRGs) (13). The HzRGs routinely exhibit giant ~100 kpc nebulae of luminous Lyman-α (Lyα) emission $L_{\mathrm{Ly\alpha}} \sim 10^{44}\ \mathrm{erg\ s}^{-1}$. Nebulae of comparable size and luminosity have also been observed in a distinct population of objects known as Lyα blobs (LABs) (14, 15). The LABs are also frequently associated with AGN activity (16–18), although lacking powerful radio jets, and appear to reside in overdense protocluster environments (15, 19, 20). Thus, among the handful of protoclusters (21) known, most appear to share two common characteristics: the presence of an active SMBH and a giant Lyα nebula.

We have recently completed a spectroscopic search for extended Lyα emission around a sample of 29 luminous quasars at $z \sim 2$, each the foreground (f/g) member of a projected quasar pair (22). Analysis of spectra from the background (b/g) members in such pairs reveals that quasars exhibit frequent absorption from a cool, metal-enriched, and often optically thick medium on scales of tens to hundreds of kiloparsecs (22–28). The ultraviolet radiation emitted by the luminous f/g quasar can, like a flashlight, illuminate this nearby neutral hydrogen and power a large-scale Lyα-emission nebula, motivating our search. By construction, our survey selects for exactly the two criteria that seem to strongly correlate with protoclusters: an active SMBH and the presence of a large-scale Lyα emission nebula.

Of the 29 quasars surveyed, only SDSSJ0841+3921 exhibited extended large-scale (≳50 kpc) Lyα emission above our characteristic sensitivity limit of $6 \times 10^{-18}\ \mathrm{erg\ s}^{-1}\ \mathrm{cm}^{-2}\ \mathrm{arc\ sec}^{-2}$ (2s). We designed a custom narrow-band filter tuned to

[1]Max-Planck-Institut für Astronomie, Heidelberg, Germany. [2]University of California Observatories–Lick Observatory, University of California Santa Cruz, Santa Cruz, CA, USA. [3]ETH Zurich, Institute for Astronomy, Zurich, Switzerland.
*Corresponding author. E-mail: joe@mpia.de

(Cold) Dark Matter does not exist!

Journal of Cosmology (2015), Vol. 24, No. 46, pp 12731-12739.

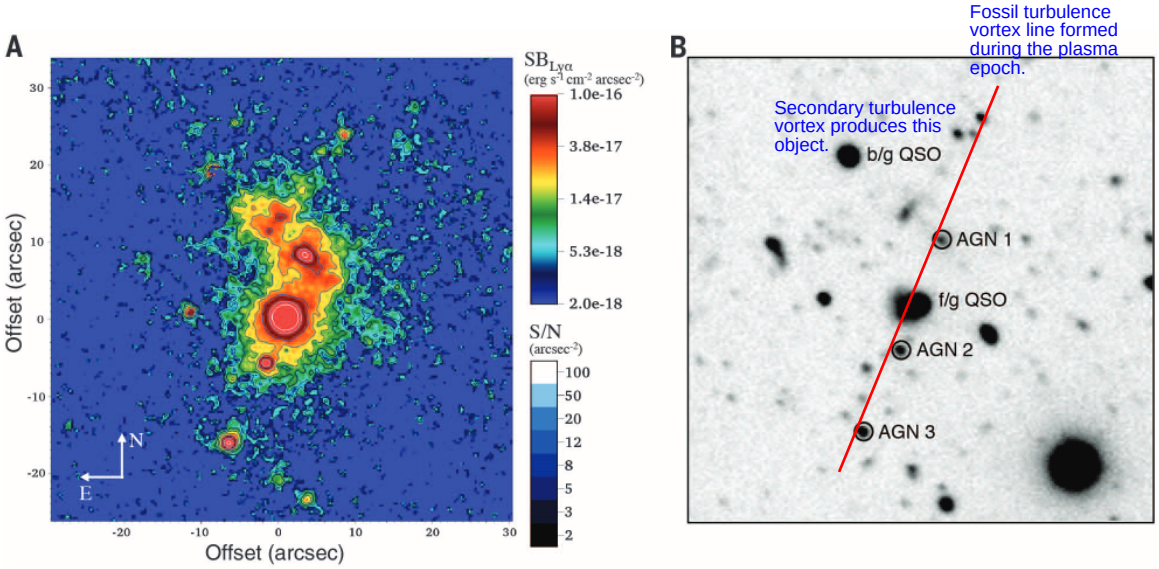

Fig. 1. Narrow- and broadband images of the field surrounding SDSSJ0841+3921 (A) Continuum-subtracted, narrow-band image of the field around f/g quasar. The color map and the contours indicate the Lya surface brightness (upper color bar) and the signal-to-noise ratio per arc sec^2 aperture (lower color bar), respectively. This image reveals a giant Lya nebula on the northern side of the f/g quasar and several compact bright Lya emitters in addition to the f/g quasar. Three of these have been spectroscopically confirmed as AGNs at the same redshift. (B) Corresponding V-band continuum image of the field presented at left with the locations of the four AGNs marked. The AGNs are roughly oriented along a line coincident with the projected orientation of the Lya nebula. We also mark the position of the b/g quasar, which is not physically associated with the quadruple AGN system but whose absorption spectrum probes the gaseous environment of the f/g quadruple AGN and protocluster (Fig. 4).

the wavelength of Lyα at the f/g quasar redshift z = 2.0412 (central wavelength = 3700 Å, full width at half maximum = 33 Å), and imaged the field with the Keck/LRIS imaging spectrometer for 3 hours on UT 12 November 2012. The combined and processed images reveal Lyα emission from a giant filamentary structure centered on the f/g quasar and extending continuously toward the b/g quasar (Fig. 1). This nebulosity has an end-to-end size of 37″, corresponding to 310 kpc, and a total line luminosity $L_{Ly\alpha} = 2.1 \times 10^{44}$ erg s^{-1}, making it one of the largest and brightest nebulae ever discovered.

The giant nebula is only one of the exceptional properties of SDSSJ0841+3921. Our images reveal three relatively compact candidate Lyα-emitting sources with faint continuum magnitudes V ≃ 23 to 24, embedded in the Lyα filament and roughly aligned with its major axis. Followup spectroscopy reveals that the sources labeled AGN1, AGN2, and AGN3 are three AGNs at the same redshift as the f/g quasar [see the right panel of Fig. 1 and (29)], making this system the only quadruple AGN known. Adopting recent measurements of small-scale quasar clustering (30), we estimate that the probability of finding three AGNs around a quasar with such small separations is ~10^{-7} (31). Why then did we discover this rare coincidence of AGNs in a survey of just 29 quasars? Did the giant nebula mark the location of a protocluster with dramatically enhanced AGN activity?

To test this hypothesis, we constructed a catalog of Lyα-emitting galaxies (LAEs) and computed the cumulative overdensity profile of LAEs around SDSSJ0841+3921, relative to the background number expected based on the LAE luminosity function (32) (Fig. 2). To perform a quantitative comparison to other giant Lyα nebulae, many of which are known to coincide with protoclusters, we measured the giant nebulae–LAE cross-correlation function for a sample of eight systems—six HzRGs and two LABs—for which published data was available in the literature (33). In Fig. 2, we compare the overdensity profile around SDSSJ0841+3921 to this giant nebulae–LAE correlation function. On average, the environment of HzRGs and LABs hosting giant Lyα nebulae (red line) is much richer than that of radio-quiet quasars (10) (blue line), confirming that they indeed reside in protoclusters. Furthermore, the clustering of LAEs around SDSSJ0841+3921 has a steeper overdensity profile and exceeds the average protocluster

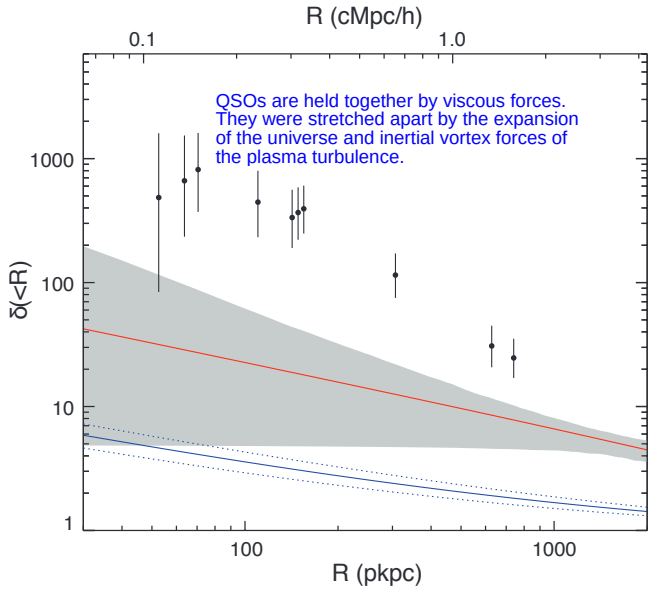

Fig. 2. Characterization of the protocluster environment around SDSSJ0841+3921. The data points indicate the cumulative overdensity profile of LAEs d(<R) as a function of impact parameter R from the f/g quasar in SDSSJ0841+3921, with Poisson error bars. The red curve shows the predicted overdensity profile, based on our measurement of the giant nebulae–LAE cross-correlation function determined from a sample of eight systems—six HzRGs and two LABs—for which published data were available in the literature. Assuming a power-law form for the cross-correlation $x_{cross} = (r/r_0)^{-g}$, we measured the correlation length $r_0 = 29.3 \pm 4.9$ h^{-1} Mpc, for a fixed value of g = 1.5. The gray-shaded region indicates the 1s error on our measurements based on a bootstrap analysis, where both r_0 and g are allowed to vary. The solid blue line indicates the overdensity of Lyman break galaxies (LBGs) around radio-quiet quasars based on recent measurements (10), with the dotted blue lines the 1s error on this measurement. On average, the environment of HzRGs and LABs hosting giant Lya nebulae is much richer than that of radio-quiet quasars (10), confirming that they indeed reside in protoclusters. SDSSJ0841+3921 exhibits a dramatic excess of LAEs as compared to the expected overdensities around radio-quiet quasars (blue curve). Its overdensity even exceeds the average protocluster (red curve) by a factor of ≳20 for R < 200 kpc, decreasing to an excess of ~3 on scales of R ≃ 1 Mpc, and exhibits a much steeper profile.

Viscous and inertial vortex forces force protogalaxies back toward the primary turbulent vortex that triggers the galaxy formation by its large rate-of-strain. The secondary vortices move galaxies away. See Journal of Cosmology (2015) Vol. 24 discussion of Stephan's Quintet.

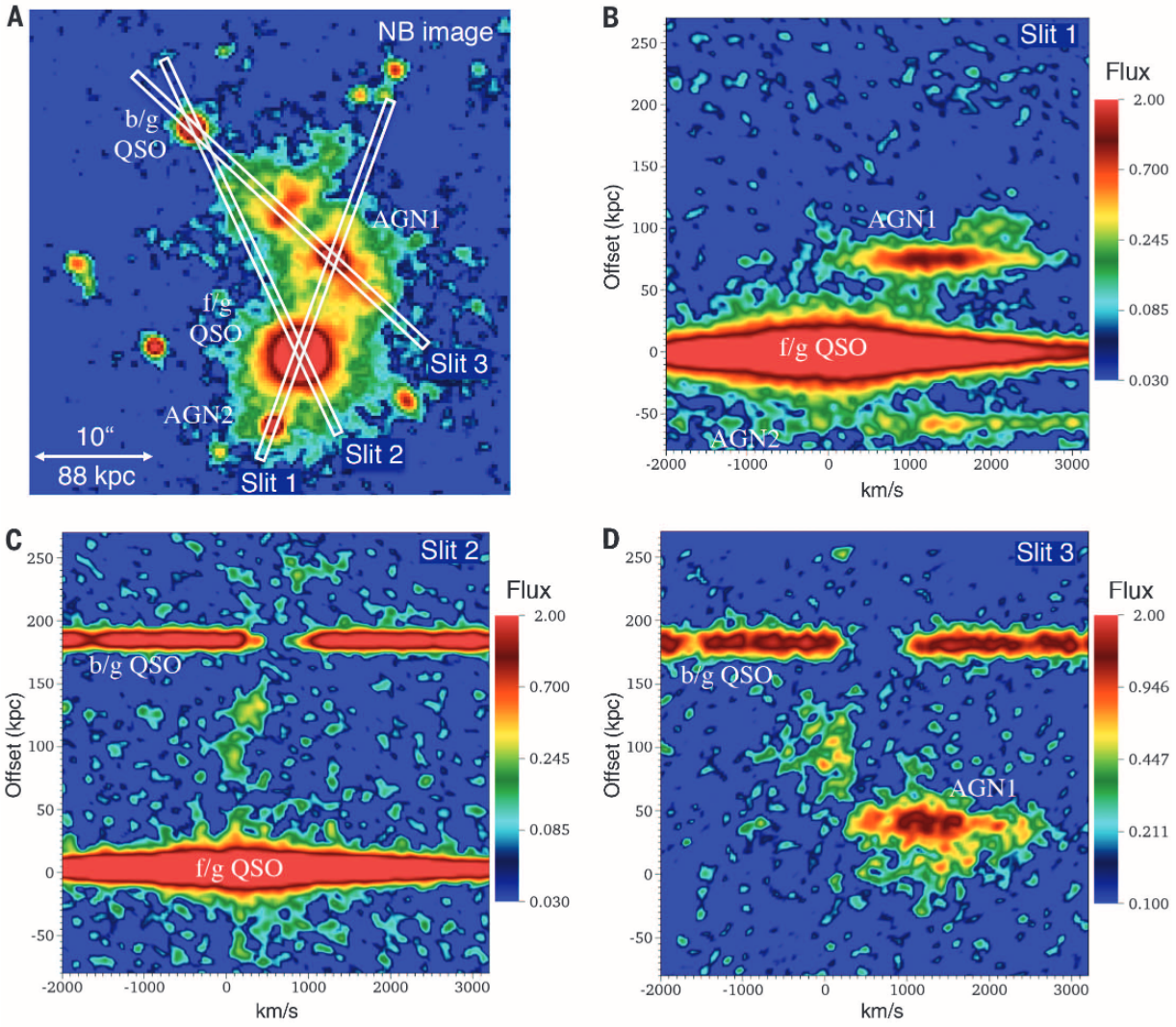

Fig. 3. Lyα spectroscopy of the giant nebula and its associated AGNs. (A) The spectroscopic slit locations (white rectangles) for three different slit orientations are overlaid on the narrowband image of the giant nebula. The locations of the f/g quasar (brightest source), b/g quasar, AGN1, and AGN2 are also indicated. Two-dimensional spectra for slit1 (B), slit2 (C), and slit3 (D) are shown in the accompanying panels. In the upper right and lower left panels, spatial coordinates refer to the relative offset along the slit with respect to the f/g quasar. Spectra of AGN1 are present in both slit 1 (upper right) and slit 3 (lower right) at spatial offsets of 75 and 25 kpc, respectively, whereas the Lyα spectrum of AGN2 is located at a spatial offset −60 kpc in slit 1 (upper right). The b/g quasar spectra are located in both slit 2 (lower left) and slit 3 (lower right) at the same spatial offset of 176 kpc. The spectroscopic observations demonstrate the extreme kinematics of the system: AGN1 has a velocity of +1300 ± 400 km s^{-1} relative to the f/g quasar, and the Lyα emission in the nebula exhibits motions ranging from −800 km s^{-1} (at ≈100 kpc offset in slit 3, lower right) to +2500 km s^{-1} (at ≈100 kpc in slit 1, upper right). A 3 × 3 pixel boxcar smoothing, which corresponds to 120 km s^{-1} × 0.8″, has been applied to the spectra. In each two-dimensional spectrum, the zero velocity corresponds to the systemic redshift of the f/g quasar. The color bars indicate the flux levels in units of erg s^{-1} cm^{-2} arc sec^{-2} Å^{-1}.

by a factor of ≳20 for $R < 200$ kpc and by ~ 3 on scales of $R \simeq 1$ Mpc. In addition to the overdensity of four AGNs, the high number of LAEs surrounding SDSSJ0841+3921 make it one of the most overdense protoclusters known at $z \sim 2$ to 3.

The combined presence of several bright AGNs, the Lyα emission nebula, and the b/g absorption spectrum provides an unprecedented opportunity to study the morphology and kinematics of the protocluster via multiple tracers, and we find evidence for extreme motions (34). Specifically, AGN1 is offset from the precisely determined systemic redshift (35) of the f/g quasar by +1300 ± 400 km s^{-1}. This large velocity offset cannot be explained by Hubble expansion [the miniscule probability of finding a quadruple quasar in the absence of clustering $P \sim 10^{-13}$ (31) and the physical association between the AGN and giant nebula demand that the four AGNs reside in a real collapsed structure] and thus provides unambiguous evidence for extreme gravitational motions. In addition, our slit spectra of the giant Lyα nebula reveal extreme kinematics of diffuse gas (Fig. 3), extending over a velocity range of −800 to +2500 km s^{-1} from systemic. Furthermore, there is no evidence for the double-peaked velocity profiles characteristic of resonantly trapped Lyα, which could generate large velocity widths in the absence of correspondingly large gas motions. Absorption line kinematics of the metal-enriched gas, measured from the b/g quasar spectrum at an impact parameter of $R_\perp = 176$ kpc (Fig. 4), show strong absorption at ≈+650 km s^{-1}, with a significant tail to velocities as large as ≃1000 km s^{-1}. It is of course possible that the extreme gas kinematics, traced by Lyα emission and metal-line absorption, are not gravitational but rather arise from violent large-scale outflows powered by the multiple AGNs. Although we cannot completely rule out this possibility, the large velocity offset of +1300 km s^{-1} between the f/g quasar and the emission redshift of AGN1 can only result from gravity.

One can only speculate about the origin of the dramatic enhancement of AGNs in the SDSSJ0841+3921 protocluster. Perhaps the duty cycle for

Journal of Cosmology (2015), Vol. 24, No. 46, pp 12731-12739.

AGN activity is much longer in protoclusters, because of frequent dissipative interactions (5, 6), or an abundant supply of cold gas. A much larger number of massive galaxies could also be the culprit, as AGNs are known to trace massive halos at $z \sim 2$. Although SDSSJ0841+3921 is the only example of a quadruple AGN with such small separations, previously studied protoclusters around HzRGs and LABs also occasionally harbor multiple AGNs (13, 36). Regardless, our discovery of a quadruple AGN and protocluster from a sample of only 29 quasars suggests a link between giant Lyα nebulae, AGN activity, and protoclusters, similar to past work on HzRGs and LABs, with the exception that SDSSJ0841+3921 was selected from a sample of normal radio-quiet quasars. From our survey and other work (37), we estimate that ≃10% of quasars exhibit comparable giant Lyα nebulae. Although clustering measurements imply that the majority of $z \sim 2$ quasars reside in moderate overdensities (10–12), we speculate that this same 10% trace much more massive protoclusters. SDSSJ0841+3921 clearly supports this hypothesis, as does another quasar-protocluster association (10, 38), around which a giant Lyα nebula was recently discovered (39, 40).

Given our current theoretical picture of galaxy formation in massive halos, an association between giant Lyα nebulae and protoclusters is completely unexpected. The large Lyα luminosities of these nebulae imply a substantial mass ($\sim 10^{11}\ M_\odot$) of cool ($T \sim 10^4$ K) gas (41), whereas cosmological hydrodynamical simulations indicate that already by $z \sim 2$ to 3, baryons in the massive progenitors ($M_{halo} \gtrsim 10^{13}\ M_\odot$) of present-day clusters are dominated by a hot shock-heated plasma $T \sim 10^7$ K (42, 43). These hot halos are believed to evolve into the x-ray–emitting intracluster medium observed in clusters, for which absorption-line studies indicate negligible ≲1% cool gas fractions (44). Clues about the nature of this apparent discrepancy come from our absorption line studies of the massive $\simeq 10^{12.5}\ M_\odot$ halos hosting $z \sim 2$ to 3 quasars. This work reveals substantial reservoirs of cool gas $\gtrsim 10^{10}\ M_\odot$ (22–28), manifest as a high covering factor ≃50% of optically thick absorption, several times larger than predicted by hydrodynamical simulations (42, 43). This conflict most likely indicates that current simulations fail to capture essential aspects of the hydrodynamics in massive halos at $z \sim 2$ (27, 42), perhaps failing to resolve the formation of clumpy structure in cool gas (41).

If illuminated by the quasar, these large cool gas reservoirs in the quasar circumgalactic medium (CGM) will emit fluorescent Lyα photons, and we argue that this effect powers the nebula in SDSSJ0841+3921 (45). But according to this logic, nearly every quasar in the universe should be surrounded by a giant Lyα nebula with size comparable to its CGM (~200 kpc). Why then are these giant nebulae not routinely observed?

This apparent contradiction can be resolved as follows. If this cool CGM gas is illuminated and highly ionized, it will fluoresce in the Lyα line with a surface brightness scaling as $SB_{Lya} \propto N_H n_H$, where N_H is the column density of cool gas clouds that populate the quasar halo, and n_H is the number density of hydrogen atoms inside these clouds. The total cool gas mass of the halos scales as $M_{cool} \propto R^2 N_H$, where R is the radius of the halo (45). Given our best estimate for the properties of the CGM around typical quasars ($n_H \sim 0.01\ cm^{-3}$ and $N_H \sim 10^{20}\ cm^{-2}$ or $M_{cool} \simeq 10^{11}\ M_\odot$) (22, 26, 27), we expect these nebulae to be extremely faint $SB_{Lya} \sim 10^{-19}$ erg s^{-1} cm^{-2} arc sec^{-2} and beyond the sensitivity of current instruments (22). One comes to a similar conclusion based on a full radiative transfer calculation through a simulated dark-matter halo with mass $M_{halo} \approx 10^{12.5}\ M_\odot$ (41). Thus the factor of ~100 times larger surface brightness observed in the SDSSJ0841+3921 and other protocluster nebulae arises from either a higher n_H, N_H (and hence higher M_{cool}), or both. The cool gas properties required to produce the SDSSJ0841+3921 nebula can be directly compared to those deduced from an absorption line analysis of the b/g quasar spectrum (46).

The b/g quasar sightline pierces through SDSSJ0841+3921 at an impact parameter of $R_\perp = 176$ kpc, giving rise to the absorption spectrum shown in Fig. 4. Photoionization modeling of these data constrains the total hydrogen column density to be $\log_{10} N_H = 20.4 \pm 0.4$ (45), implying a substantial mass of cool gas $1.0 \times 10^{11}\ M_\odot < M_{cool} < 6.5 \times 10^{11}\ M_\odot$ within $r = 250$ kpc. Assuming that the Lyα emitting gas has the same column density as the gas absorbing the b/g sightline, reproducing the large fluorescent Lyα surface brightness requires that this gas be distributed in compact $r_{cloud} \sim 40$ pc clouds at densities characteristic of the interstellar medium $n_H \simeq 2\ cm^{-3}$, but on ~100-kpc scales in the protocluster.

Clues to the origin of these dense clumps of cool gas come from their high enrichment level, which we have determined from our absorption line analysis (46) to be greater than 1/10th of the solar value. At first glance, this suggests that strong tidal interactions due to merger activity or

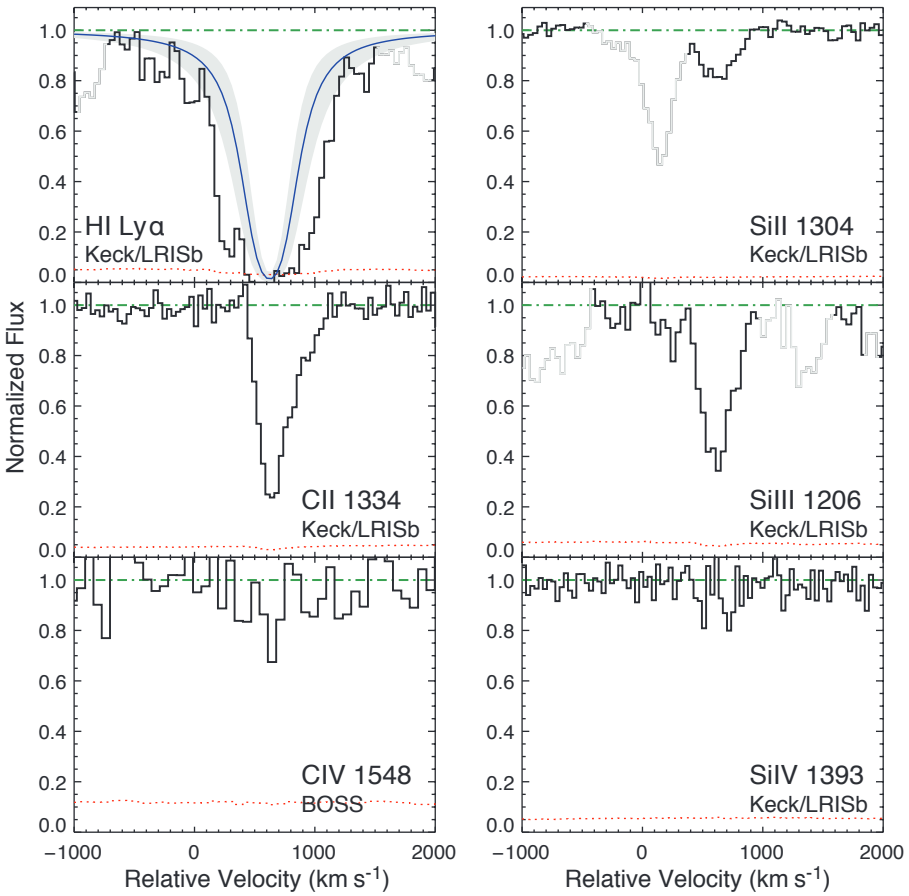

Fig. 4. Absorption line spectrum of cool gas in SDSSJ0841+3921. The spectrum of the absorbing gas detected in the b/g quasar sightline at an impact parameter of 176 kpc from the f/g quasar is shown. The gas shows strong HI and low-ionization–state metal absorption, offset by ≈650 km s^{-1} from the f/g quasar's systemic redshift. The CII absorption in particular exhibits a significant tail to velocities as large as ≃1000 km s^{-1}, providing evidence for extreme gas kinematics. We modeled the strong HI Lyα absorption with a Voigt profile (blue curve with gray band indicating uncertainty) and estimate a column density $\log N_{HI} = 19.2 \pm 0.3$. The strong low and intermediate ion absorption (SiII, CII, and SiIII) and correspondingly weak high ion absorption (CIV and SiIV) indicate that the gas is not highly ionized, and our photoionization modeling (45) implies $\log_{10} x_{HI} = -1.2 \pm 0.3$ or $\log_{10} N_H = 20.4 \pm 0.4$. We estimate a conservative lower limit on the gas metallicity to be 1/10th of the solar value. Spectral regions contaminated by other unassociated absorption are indicated in light gray.

outflows due to powerful AGN feedback are responsible for dispersing dense cool gas in the protocluster. However, the large cool gas mass $\sim 10^{11}\ M_\odot$ and high velocities ~1000 km s^{-1} imply an extremely large kinetic luminosity $L_{wind} \sim 10^{44.6}$ for an AGN-powered wind, making the feedback scenario implausible (25). An even more compelling argument against a merger or feedback origin comes from the extremely small cloud sizes $r_{cloud} \sim$ 40 pc implied by our measurements. Such small clouds moving supersonically ~1000 km s^{-1} through the hot $T \sim 10^7$ K shock-heated plasma predicted to permeate the protocluster will be disrupted by hydrodynamic instabilities in $\sim 5 \times 10^6$ years and can thus only be transported ~5 kpc (47). These short disruption time scales instead favor a scenario where cool dense clouds are formed in situ, perhaps via cooling and fragmentation instabilities, but are short-lived. The higher gas densities might naturally arise if hot plasma in the incipient intracluster medium pressure-confines the clouds, compressing them to high densities (48, 49). Emission line nebulae from cool dense gas have also been observed at the centers of present-day cooling flow clusters (50, 51), albeit on much smaller scales ≲50 kpc. The giant Lyα nebulae in $z \sim 2$ to 3 protoclusters might be manifestations of the same phenomenon, but with much larger sizes and luminosities, reflecting different physical conditions at high redshift.

The large reservoir of cool dense gas in the protocluster SDSSJ0841+3921, as well as those implied by the giant nebulae in other protoclusters, appear to be at odds with our current theoretical picture of how clusters form. This is likely to be symptomatic of the same problem of too much cool gas in massive halos already highlighted for the quasar CGM (27, 42, 43). Progress will require more cosmological simulations of massive halos $M \gtrsim 10^{13}\ M_\odot$ at $z \sim 2$, as well as idealized higher-resolution studies. In parallel, a survey for extended Lyα emission around ~100 quasars would uncover a sample of ~10 giant Lyα nebulae, likely coincident with protoclusters, possibly also hosting multiple AGNs, and enabling continued exploration of the relationship between AGNs, cool gas, and cluster progenitors.

REFERENCES AND NOTES

1. J. Magorrian et al., Astron. J. 115, 2285–2305 (1998).
2. L. Ferrarese, Astrophys. J. 578, 90–97 (2002).
3. J. N. Bahcall, S. Kirhakos, D. H. Saxe, D. P. Schneider, Astrophys. J. 479, 642–658 (1997).
4. M. G. Haehnelt, M. J. Rees, Mon. Not. R. Astron. Soc. 263, 168–178 (1993).
5. S. Djorgovski, The Space Distribution of Quasars, D. Crampton, Ed., vol. 21 of Astronomical Society of the Pacific Conference Series (Astronomical Society of the Pacific, San Franscisco, 1991), pp. 349–353.
6. J. F. Hennawi et al., Astron. J. 131, 1–23 (2006).
7. S. G. Djorgovski et al., Astrophys. J. 662, L1–L5 (2007).
8. E. P. Farina, C. Montuori, R. Decarli, M. Fumagalli, Mon. Not. R. Astron. Soc. 431, 1019–1025 (2013).
9. C. Lacey, S. Cole, Mon. Not. R. Astron. Soc. 262, 627–649 (1993).
10. R. F. Trainor, C. C. Steidel, Astrophys. J. 752, 39 (2012).
11. M. White et al., Mon. Not. R. Astron. Soc. 424, 933–950 (2012).
12. N. Fanidakis, A. V. Macciò, C. M. Baugh, C. G. Lacey, C. S. Frenk, Mon. Not. R. Astron. Soc. 436, 315–326 (2013).
13. B. P. Venemans et al., Astron. Astrophys. 461, 823–845 (2007).
14. P. J. Francis et al., Astrophys. J. 457, 490 (1996).
15. C. C. Steidel et al., Astrophys. J. 532, 170–182 (2000).
16. A. Dey et al., Astrophys. J. 629, 654–666 (2005).
17. R. A. Overzier et al., Astrophys. J. 771, 89 (2013).
18. M. K. M. Prescott, I. Momcheva, G. B. Brammer, J. P. U. Fynbo, P. Møller, Astrophys. J. 802, 32 (2015).
19. M. K. M. Prescott, N. Kashikawa, A. Dey, Y. Matsuda, Astrophys. J. 678, L77–L80 (2008).
20. Y. Yang, A. Zabludoff, C. Tremonti, D. Eisenstein, R. Davé, Astrophys. J. 693, 1579–1587 (2009).
21. Y.-K. Chiang, R. Overzier, K. Gebhardt, Astrophys. J. 779, 127 (2013).
22. J. F. Hennawi, J. X. Prochaska, Astrophys. J. 766, 58 (2013).
23. J. F. Hennawi et al., Astrophys. J. 651, 61–83 (2006).
24. J. F. Hennawi, J. X. Prochaska, Astrophys. J. 655, 735–748 (2007).
25. J. X. Prochaska, J. F. Hennawi, Astrophys. J. 690, 1558–1584 (2009).
26. J. X. Prochaska, J. F. Hennawi, R. A. Simcoe, Astrophys. J. 762, L19 (2013).
27. J. X. Prochaska et al., Astrophys. J. 776, 136 (2013).
28. J. X. Prochaska, M. W. Lau, J. F. Hennawi, Astrophys. J. 796, 140 (2014).
29. See supplementary text S2.
30. I. Kayo, M. Oguri, Mon. Not. R. Astron. Soc. 424, 1363–1371 (2012).
31. See supplementary text S3.
32. R. Ciardullo et al., Astrophys. J. 744, 110 (2012).
33. See supplementary text S4.
34. See supplementary text S6.
35. See supplementary text S5.
36. B. D. Lehmer et al., Astrophys. J. 691, 687–695 (2009).
37. See supplementary text S7.
38. R. E. Mostardi et al., Astrophys. J. 779, 65 (2013).
39. D. C. Martin et al., Astrophys. J. 786, 106 (2014).
40. See supplementary text S8.
41. S. Cantalupo, F. Arrigoni-Battaia, J. X. Prochaska, J. F. Hennawi, P. Madau, Nature 506, 63–66 (2014).
42. M. Fumagalli et al., Astrophys. J. 780, 74 (2014).
43. C.-A. Faucher-Giguere et al., Mon. Not. R. Astron. Soc. 449, 987–1003 (2015).
44. S. Lopez et al., Astrophys. J. 679, 1144–1161 (2008).
45. See supplementary text S9.
46. See supplementary text S10.
47. N. H. M. Crighton et al., Mon. Not. R. Astron. Soc. 446, 18–37 (2015).
48. A. H. Maller, J. S. Bullock, Mon. Not. R. Astron. Soc. 355, 694–712 (2004).
49. H. J. Mo, J. Miralda-Escude, Astrophys. J. 469, 589 (1996).
50. T. M. Heckman, S. A. Baum, W. J. M. van Breugel, P. McCarthy, Astrophys. J. 338, 48 (1989).
51. M. McDonald, S. Veilleux, D. S. N. Rupke, R. Mushotzky, Astrophys. J. 721, 1262–1283 (2010).

ACKNOWLEDGMENTS

We thank the staff of the W. M. Keck Observatory for their support during the installation and testing of our custom-built narrow-band filter. We are grateful to B. Venemans and M. Prescott for providing us with catalogs of LAE positions around giant nebulae in electronic format. We also thank the members of the ENIGMA group (http://www.mpia-hd.mpg.de/ENIGMA/) at the Max Planck Institute for Astronomy for helpful discussions. J.F.H. acknowledges generous support from the Alexander von Humboldt foundation in the context of the Sofja Kovalevskaja Award. The Humboldt foundation is funded by the German Federal Ministry for Education and Research. J.X.P. acknowledges support from NSF grant AST-1010004. The data presented here were obtained at the W. M. Keck Observatory, which is operated as a scientific partnership among the California Institute of Technology, the University of California, and NASA. The observatory was made possible by the financial support of the W. M. Keck Foundation. We acknowledge the cultural role that the summit of Mauna Kea has within the indigenous Hawaiian community. We are most fortunate to have the opportunity to conduct observations from this mountain. The data reported in this paper are available through the Keck Observatory Archive.

SUPPLEMENTARY MATERIALS

www.sciencemag.org/content/348/6236/779/suppl/DC1
Materials and Methods
Supplementary Text
Figs. S1 to S10
Tables S1 to S6
References (52–133)

22 December 2014; accepted 2 April 2015
10.1126/science.aaa5397

To summarize, the observations leave no doubt that the Quasar Quartet is closely related to the Gibson and Schild 2007 discussion of Stephan's Quintet. The Quartet can be interpreted as an early version of the Quintet: baby pictures of strings of galaxies produced by turbulence when the plasma was capable of fragmentation into protogalaxies. Both primary and secondary vortices are shown by the Quintet in the figure. CHG